Specific Inhibition of MicroRNA Processing Using L-RNA Aptamers

Jonathan T. Sczepanski[†] and Gerald F. Joyce*

Department of Chemistry and The Skaggs Institute for Chemical Biology, The Scripps Research Institute, 10550 North Torrey Pines Road, La Jolla, California 92037, United States

S Supporting Information

ABSTRACT: *In vitro* selection was used to obtain L-RNA aptamers that bind the distal stem-loop of various precursor microRNAs (pre-miRs). These L-aptamers, termed "aptamiRs", bind their corresponding pre-miR target through highly specific tertiary interactions rather than Watson–Crick pairing. Formation of a pre-miR–aptamiR complex inhibits Dicer-mediated processing of the pre-miR, which is required to form the mature functional microRNA. One of the aptamiRs, which was selected to bind oncogenic pre-miR-155, inhibits Dicer processing under simulated physiological conditions, with an IC_{50} of 87 nM. Given that L-RNAs are intrinsically resistant to nuclease degradation, these results suggest that aptamiRs might be pursued as a new class of miR inhibitors.
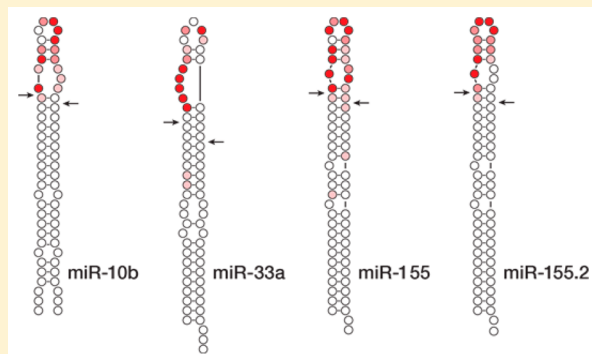
INTRODUCTION

MicroRNAs (miRs) are small, noncoding RNAs that act as post-transcriptional regulators of gene expression.[1] miRs are involved in many important biological processes, including development, differentiation, and apoptosis, and alterations in their expression patterns can contribute to the pathogenesis of human disease.[2]

The biogenesis of miRs is a multistep process, which begins in the nucleus with the synthesis of a primary RNA transcript (pri-miR). The pri-miR is cleaved by the nuclear endoribonuclease Drosha to form a precursor miR (pre-miR), which has an extended stem–loop structure. The pre-miR then is exported to the cytoplasm, where the type III ribonuclease Dicer excises the distal portion of the stem–loop. This results in a mature double-stranded miR that is loaded onto Argonaute protein and used to guide the sequence-specific silencing of complementary mRNA targets.

Because of the many important biological roles of miRs, considerable effort has been made to develop tools for silencing particular miRs, both to investigate their function and to develop potential therapeutic agents. The most widely used strategy for miR-specific silencing employs antisense oligonucleotides (ASOs).[3] These ASO-based inhibitors are designed to hybridize via Watson–Crick pairing to the mature miR of interest, presumably after it has assembled with Argonaute protein, thereby preventing the RNA component of the silencing complex from binding to its mRNA targets. For most applications, ASOs are comprised of nuclease-resistant oligonucleotide analogues, such as 2'-O-methyl oligonucleotides (antagomirs),[4] "locked" nucleic acids (antimiRs),[5] or peptide nucleic acids.[6] Although some degree of specificity of ASOs is assured due to the specificity of Watson–Crick pairing,

off-target effects resulting from partial complementarity to other RNAs can limit the usefulness of this approach.[7]

A more target-specific strategy for silencing miRs would employ inhibitors that recognize individual miRs or their precursors based on their unique three-dimensional shape rather than their nucleotide sequence. However, the thousands of known miRs are all processed through the same enzymatic pathway, which depends on common features of RNA structure, essentially an extended stem–loop with imperfect base pairing in the stem. This structural similarity seemingly makes the development of miR-specific inhibitors a difficult challenge.

It was recently shown that aptamers comprised of L-RNA, the enantiomer of natural D-RNA, are capable of binding structured D-RNA targets exclusively through tertiary interactions.[8] This is because D- and L-RNAs are incapable of forming contiguous Watson–Crick pairs, forcing any cross-chiral recognition to occur through tertiary interactions.[9] Motivated by these earlier findings, the present study demonstrates the ability of L-aptamers to bind tightly and specifically to various D-miR targets that are structurally very similar, but can be distinguished based on differences of their tertiary structure. Moreover, binding of an L-aptamer to the distal stem–loop of a pre-miR inhibits Dicer-mediated cleavage, thus blocking formation of the mature miR.

RESULTS AND DISCUSSION

Three human pre-miR targets were chosen for this study: pre-miR-10b, pre-miR-33a, and pre-miR-155. miR-10b and miR-155 are prototypical oncogenic miRs, and their overexpression

has been associated with the development and invasiveness of malignancies, including leukemias and breast cancer.[2,10] miR-33a is involved in cholesterol homeostasis and fatty acid synthesis and is a potential therapeutic target for the treatment of atherosclerosis.[11]

L-RNA aptamers must initially be selected as D-aptamers against the enantiomer of the desired target,[12] which enables enzymatic amplification of the D-RNA during the process of *in vitro* selection. Therefore, it was necessary to prepare L-RNA versions of each pre-miR target by chemical synthesis using commercially available L-nucleoside phosphoramidites. The proximal stem portion of each L-pre-miR was truncated to direct binding of the aptamers to the distal stem—loop (Figure 1a).
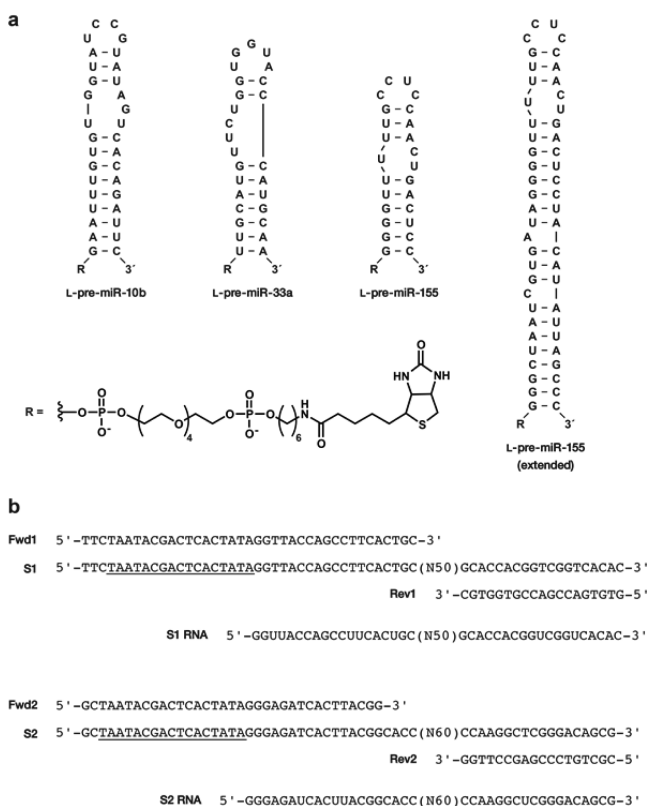

Figure 1. Materials used for *in vitro* selection of aptamiRs. (a) Sequence and secondary structure of truncated L-pre-miR-10b, L-pre-miR-33a, and L-pre-miR-155, and of extended-length L-pre-miR-155. (b) Sequences of the two pools of synthetic DNA molecules (S1 and S2), containing either 50 (N50) or 60 (N60) random-sequence nucleotides, flanked by binding sites for forward (Fwd1 or Fwd2) and reverse (Rev1 or Rev2) primers. The T7 RNA polymerase promoter sequence is underlined. Corresponding pools of RNAs contain either 50 or 60 random-sequence nucleotides flanked by fixed primer sites.

Two starting pools of D-RNAs were constructed, one containing 50 and the other containing 60 random-sequence nucleotides, each flanked by fixed primer-binding sites (Figure 1b). *In vitro* selection was carried out separately for each of the three pre-miR targets, except during the first four rounds when both pre-miR-10b and pre-miR-33a were present in the same mixture. The pool of RNAs were incubated together with the 5′-biotinylated L-pre-miR target in a mixture containing either 5 mM MgCl$_2$ (for pre-miR-10b and pre-miR-33a) or 10 mM MgCl$_2$ (for pre-miR-155), 150 mM NaCl, 0.1% TWEEN 20,

and 25 mM Tris (pH 7.6) at 23 °C. D-RNA molecules that bound the L-pre-miR target were captured using streptavidin-coated magnetic beads and subsequently washed with the binding solution. Aptamers that remained bound then were eluted using 25 mM NaOH, reverse transcribed, and amplified by PCR. The resulting DNAs were used to transcribe a corresponding pool of D-RNA molecules to begin the next round of *in vitro* selection.

A total of six rounds were carried out against L-pre-miR-33a and L-pre-miR-155, and seven rounds were carried out against L-pre-miR-10b. The selection pressure was increased during successive rounds by gradually increasing the duration of the washing steps and by decreasing the concentrations of both the population of D-RNAs and the target L-pre-miR. The progress of the selection procedure was monitored informally by noting the yield of PCR products obtained during each round of selection. Following the final round, individual RNAs were cloned from the population and sequenced (see Supporting Information, Figure S1a–c).

Several clones from each population were analyzed for binding to their cognate L-pre-miR using an electrophoretic mobility-shift assay (EMSA). The highest affinity clone from each population was trimmed of extraneous nucleotides, and the corresponding L-RNA aptamer was prepared by solid-phase synthesis. The resulting L-aptamers, termed aptamiRs, were tested for their ability to bind full-length D-pre-miR targets. Not surprisingly, each aptamiR has a unique sequence and predicted secondary structure, which reflects its ability to bind to a structurally distinct pre-miR target (Figure 2). The K_d values of aptamiR-10b, aptamiR-33a, and aptamiR-155 for their cognate pre-miRs are 20, 44, and 19 nM, respectively. No binding was detected between these aptamiRs and the noncognate pre-miRs, even at 1 μM aptamiR concentration (Figure 3a,c).

The L-aptamers were predicted to bind the distal stem—loop of the pre-miRs because this region offered the best opportunity to contact unpaired nucleotides. To investigate this possibility, partial self-cleavage experiments were carried out, comparing the pre-miRs either alone or when bound by the aptamiR. The spontaneous self-cleavage of RNA is dependent on accessing an in-line geometry between the 2′-hydroxyl and vicinal phosphate at the site of strand scission.[13] Therefore, structured RNA regions tend to be less susceptible to self-cleavage compared to unstructured regions due to the lack of rotational freedom needed to achieve this geometry.

Incubation of each pre-miR in the presence of a saturating concentration of the corresponding aptamiR resulted in significant protection of the distal stem—loop compared to the behavior of this region in the absence of the aptamiR (Figures 2 and S2a–c). There was no protection throughout the proximal portion of the pre-miR stem. This suggests that the aptamiR binds the pre-miR exclusively through nucleotides in the distal loop and immediately adjacent portion of the stem.

Partial self-cleavage also was carried out for the D-RNA version of aptamiR-155, in either the presence or absence of a saturating concentration of L-pre-miR-155 (Figures 2c and S3a). This aptamiR was chosen for analysis because a second *in vitro* selection experiment was carried out for pre-miR-155 that resulted in a distinct aptamer motif, which was analyzed similarly (see below). In the bound state there was protection of the majority of the D-aptamiR-155 residues, most notably on the 5′-side of the large internal bulge loop. Taken together, the partial self-cleavage experiments suggest that aptamiR-155 binds pre-miR-155 through interactions involving a substantial
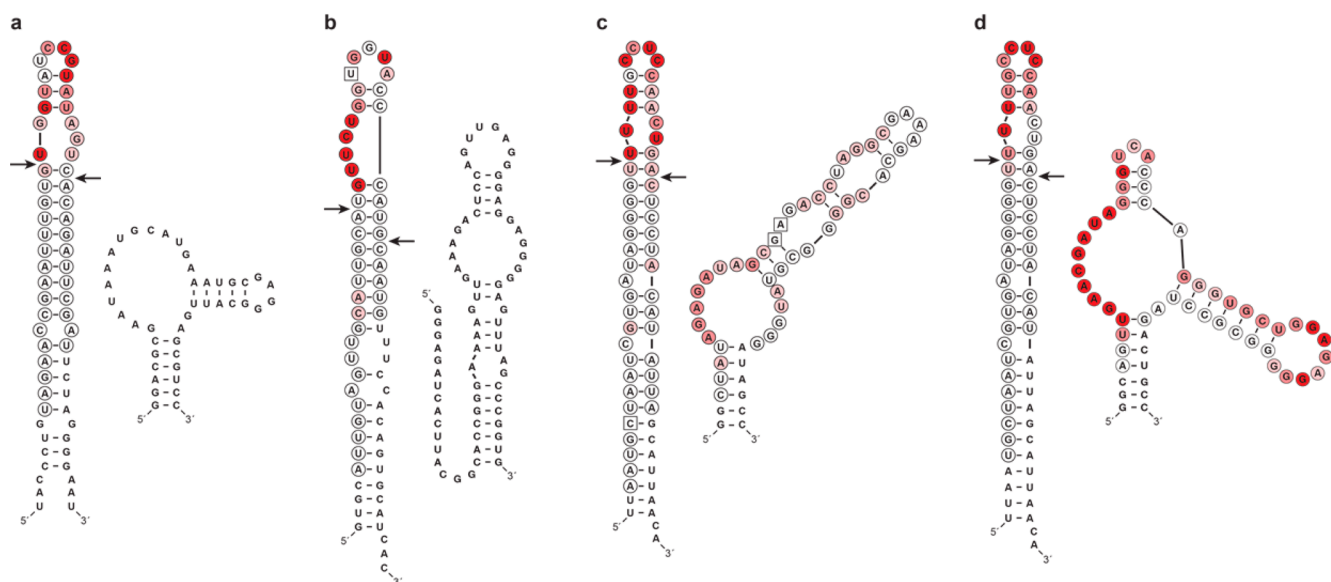
Figure 2. Sequence and secondary structure of pre-miRs and corresponding aptamiRs, showing protection of nucleotide positions against self-cleavage in the pre-miR−aptamiR complex compared to the molecules in isolation. (a) Pre-miR-10b and aptamiR-10b. (b) Pre-miR-33a and aptamiR-33a. (c) Pre-miR-155 and aptamiR-155. (d) Pre-miR-155 and aptamiR-155.2. Level of red intensity (low, medium, high) corresponds to level of protection (15−30%, 30−50%, >50%, respectively), which was determined for all circled positions. Boxes indicate nucleotide positions with increased susceptibility to self-cleavage (>30%) in the complex. Arrows indicate Dicer cleavage sites.
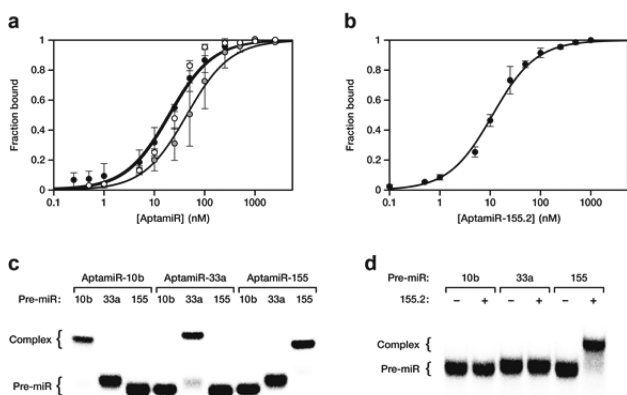

Figure 3. Binding affinity and specificity of the pre-miR−aptamiR complexes. (a) Saturation plot for binding of aptamiR-10b (white), aptamiR-33a (gray), and aptamiR-155 (black) to their corresponding pre-miRs. (b) Saturation plot for binding of aptamiR-155.2 to pre-miR-155 under simulated physiological conditions. Data were obtained in triplicate and fit to the equation: $F_{bound} = [aptamiR]/(K_d + [aptamiR])$. (c) EMSA demonstrating binding of each aptamiR to its cognate, but not noncognate, pre-miRs. All mixtures contained 0.1 nM $[5'\text{-}^{32}P]$-labeled pre-miR, 1 μM aptamiR, 5 mM $MgCl_2$, and 150 mM NaCl at pH 7.6 and 23 °C. (d) Specificity of aptamiR-155.2 for pre-miR-155, measured similarly, but in the presence of 0.5 mM $MgCl_2$ at 37 °C.

portion of the aptamer and unpaired nucleotides within the distal stem-loop of pre-miR-155.

Alteration of the distal stem-loop of pri- and pre-miRs has been shown to interfere with miR biogenesis by inhibiting cleavage by Drosha and Dicer, respectively.[14] Therefore, binding of an aptamiR to this region was expected to inhibit Dicer-mediated cleavage of the pre-miR. Pre-miR-10b, pre-miR-33a, and pre-miR-155 each were incubated in the presence of 20 nM human Dicer, together with various concentrations of the corresponding aptamiR, under reaction conditions similar

to those used during *in vitro* selection (5 mM $MgCl_2$, 100 mM NaCl, pH 7.6, 23 °C). The initial velocity of the reaction was measured in each case, and these data were used to determine the IC_{50} value for aptamiR inhibition of Dicer cleavage (Figure 4). The IC_{50} values are 32, 46, and 52 nM for aptamiR-10b,
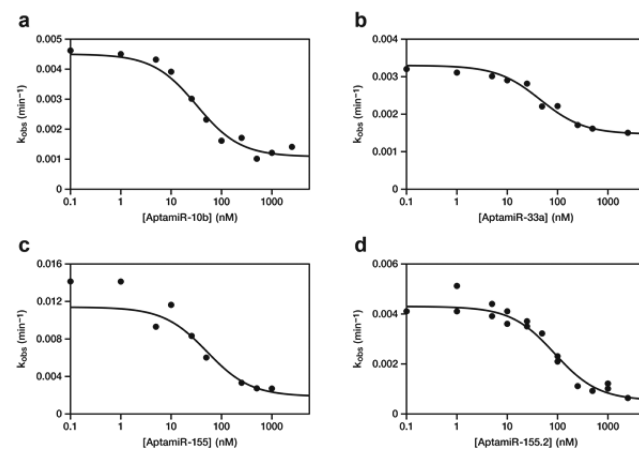

Figure 4. Inhibition of Dicer cleavage of pre-miRs by corresponding aptamiRs. (a) Pre-miR-10b and aptamiR-10b. (b) Pre-miR-33a and aptamiR-33a. (c) Pre-miR-155 and aptamiR-155. (d) Pre-miR-155 and aptamiR-155.2. Values for k_{obs} were obtained based on the initial velocity of the reaction for various concentrations of aptamiR and used to calculate IC_{50} values.

aptamiR-33a, and aptamiR-155, respectively, which are in good agreement with the corresponding K_d values determined for the pre-miR−aptamiR complexes. This suggests that formation of the complex inhibits Dicer cleavage by preventing the enzyme from binding the pre-miR. As expected, addition of 1 μM nonmatching aptamiR had no significant effect on Dicer-mediated cleavage of the pre-miR (Figure S4a−c).

In order for aptamiRs to be useful tools for inhibiting specific miRs in a biological context, they must bind their target under

physiologically relevant conditions (e.g., 0.5 mM $MgCl_2$, 150 mM KCl, pH 7.6, 37 °C), rather than the conditions that were employed during *in vitro* selection (see above). However, when tested under simulated physiological conditions, neither aptamiR-10b nor aptamiR-155 was able to bind its target. AptamiR-33a was capable of binding pre-miR-33a under these conditions, but with substantially reduced affinity (K_d = 1.3 μM; Figure S5a). These results are not surprising given the strong dependence of RNA structure on both temperature and Mg^{2+} concentration. Therefore, a second *in vitro* selection experiment was carried out against pre-miR-155 with the aim of isolating aptamiRs that function under physiologically relevant conditions. D-RNA molecules from the completed first round of the previous pre-miR-155 selection served as the starting population for this experiment.

Ten additional rounds of *in vitro* selection were carried out as before, but using an extended-length L-pre-miR-155 as the target (Figure 1a). Over the course of this selection, the concentration of Mg^{2+} was gradually reduced from 20 to 2 mM and the temperature for the binding and washing steps was increased from 23 to 37 °C. Random mutations were introduced to the population through error-prone PCR[15] after rounds four and seven. Following the 11th round of *in vitro* selection, the amplified DNA was cloned and sequenced (Figure S1d).

As before, the highest affinity clone was trimmed of extraneous nucleotides and the corresponding L-RNA aptamer, aptamiR-155.2, was prepared by solid-phase synthesis. AptamiR-155.2 shares little sequence similarity or predicted secondary structure homology with aptamiR-155 (Figure 2c,d). This suggests that binding of D-RNA by L-aptamers under physiologically relevant conditions requires different and presumably more stable RNA structures compared to L-aptamers that operate under more stabilizing conditions. In addition, these results demonstrate the importance of selecting L-aptamers under conditions relevant to their eventual use. AptamiR-155.2 binds pre-miR-155 with a K_d of 11 nM under simulated physiological conditions, as determined by EMSA (Figure 3b). The affinity of aptamiR-155.2 for pre-miR-155 is nearly unchanged under the more stabilizing selection conditions that were used previously (Figure S5b). No binding was observed between aptamiR-155.2 and the noncognate pre-miRs, even at 1 μM aptamiR concentration (Figure 3d).

As with the other aptamiRs, aptamiR-155.2 binds its pre-miR target through the distal stem–loop, as revealed by partial self-cleavage experiments (Figures 2d and S2d). The footprint of aptamiR-155.2 on pre-miR-155 is distinct from that of aptamiR-155 (Figure 2c), which likely represents differences in the specific contacts used by these two aptamers.

AptamiR-155.2 and other clones that were isolated following this *in vitro* selection procedure contain several consecutive G residues (Figure S1d). One might imagine these residues binding to the consecutive U residues on the 5′-side of the distal stem-loop of pre-miR-155 (Figure 2d). Such Watson–Crick (wobble) pairing is prohibited between D- and L-RNAs, but perhaps a contorted Watson–Crick-like geometry is possible within the context of overriding tertiary interactions. In support of this hypothesis, both the G residues of the aptamiR and the U residues of the pre-miR are protected against self-cleavage in the complex compared to the molecules in isolation. As a test, the G residues of the aptamer were mutated in pairwise fashion to A, potentially retaining Watson–Crick-like pairing, but this resulted in a complete loss of

binding (Figure S6). When instead the U residues of the aptamer were mutated to C, binding was retained for two of the four changed positions. However, when those same residues were mutated to A, binding still was preserved, suggesting that the nucleotide identity of these positions is not critical.

As a final test of the specificity of binding, both aptamiR-155.2 and the isolated clone with the second highest affinity for pre-miR-155 (clone 11-3; Figure S1d) were tested for their ability to bind the mouse homologue of pre-miR-155. The human and mouse forms differ only in the distal stem–loop, with the human pre-miR-155 having the sequence 5′-UUGCC-UCCAA-3′ and the mouse form having the sequence 5′-UGGCCUCUGA-3′ (nucleotide differences underlined). Despite these subtle differences, the aptamiRs raised against human pre-miR-155 are unable to bind the mouse homologue.

The ability of aptamiR-155.2 to inhibit Dicer-mediated cleavage of pre-miR-155 was examined under physiologically relevant conditions. Pre-miR-155 was incubated with 20 nM Dicer in a reaction mixture containing 1 mM $MgCl_2$ and 100 mM NaCl at pH 7.6 and 37 °C, together with various concentrations of aptamiR-155.2. AptamiR-155.2 exhibited concentration-dependent inhibition of pre-miR-155 cleavage, with an IC_{50} of 87 nM (Figure 4d). This value is ~8-fold higher than the observed K_d for binding of aptamiR-155.2 to pre-miR-155, which may reflect the enhanced activity of Dicer at 37 °C compared to 23 °C. In contrast, aptamiR-155 was unable to inhibit Dicer cleavage under physiologically relevant conditions. Dicer-mediated cleavage of pre-miR 10b and pre-miR 33a was not affected by the presence of aptamiR-155.2 (Figure S4d,e), again demonstrating the specificity of the pre-miR–aptamiR interaction.

■ CONCLUSIONS

Pre-miRs are generally regarded as similarly structured stem–loops with few distinguishing features. However, their individual sequences impart subtle structural differences that cause every pre-miR to adopt a unique three-dimensional shape. AptamiRs can recognize these subtle differences because RNAs of opposing chirality must interact through tertiary interactions rather than base pairing.[8] This is in contrast to D-RNA aptamers, which have a strong tendency to recognize D-RNA targets through complementary interactions,[16] and ASOs, which by design recognize their targets through Watson–Crick pairing. As a result, aptamiRs may prove to be more specific for binding their target and less susceptible to off-target interactions. Furthermore, aptamiRs do not necessarily need to overcome the local secondary structure of the target, instead adapting to the tertiary structure.

The aptamiRs described here exhibit both high affinity and high specificity for their target pre-miR. When selected to operate under physiologically relevant conditions of salt, pH, and temperature, they function accordingly. Because aptamiRs are comprised entirely of L-nucleotides, they are inherently resistant to degradation by nucleases. Thus, aptamiRs, and L-RNA aptamers in general, might be pursued as an alternative to ASOs for inhibiting the function of structured biological RNAs.

It is not clear whether the target specificity of aptamiRs observed *in vitro* will translate to the cellular context. These L-RNA molecules will not engage in Watson–Crick pairing with biological D-RNAs, but may bind off-target RNAs in an idiosyncratic manner. Furthermore, the conditions of *in vitro* selection can only simulate physiological conditions and do not reflect the exact conditions of the cellular milieu. Nonetheless,

as experience grows with L-RNA aptamers directed against protein targets, including compounds that are currently in phase II human clinical trials,[17] the opportunity to target structured RNAs with L-RNA aptamers is likely to grow.

■ EXPERIMENTAL SECTION

Materials. Oligonucleotides were either purchased from IDT (Coralville, IA) or prepared by solid-phase synthesis using an Expedite 8909 DNA/RNA synthesizer, with reagents and nucleoside phosphoramidites purchased from Glen Research (Sterling, VA), except L-2′-*tert*-butyldimethylsilyl phosphoramidites, which were from ChemGenes (Wilmington, MA). For coupling of degenerate nucleotides (N), the concentration ratios of the four nucleoside phosphoramidites A:T:G:C were 3.0:2.0:2.3:2.5, respectively, to achieve equal coupling efficiencies. All oligonucleotides were purified by denaturing polyacrylamide gel electrophoresis (PAGE) and desalted by ethanol precipitation. Histidine-tagged T7 RNA polymerase was purified from *E. coli* strain BL21 containing plasmid pBH161 (provided by William McAllister, State University of New York, Brooklyn). *Thermus aquaticus* (*Taq*) DNA polymerase was cloned from total genomic DNA and prepared as described previously.[18] Superscript II RNase H⁻ reverse transcriptase, Turbo DNase, and streptavidin-coated magnetic beads (Dynabeads, MyOne Streptavidin C1) were from Life Technologies (Carlsbad, CA). Full-length human Dicer protein was provided by Ian MacRae (The Scripps Research Institute, La Jolla, CA). Nucleoside and deoxynucleoside 5′-triphosphates were purchased from Sigma-Aldrich (St. Louis, MO) and $[\gamma\text{-}^{32}P]$ATP was from PerkinElmer (Waltham, MA).

In Vitro Selection. Libraries of dsDNAs were generated by templated extension of 300 pmol reverse primer (Rev1 or Rev2) on 200 pmol template (S1 or S2, respectively; Figure 1b) in a 50-μL reaction mixture containing 10 U/μL Superscript II reverse transcriptase, 3 mM MgCl$_2$, 75 mM KCl, 50 mM Tris (pH 8.3), and 0.25 mM each of the four dNTPs. The products of the extension reaction were added directly to a 500-μL transcription reaction containing 15 U/μL T7 RNA polymerase, 25 mM MgCl$_2$, 10 mM DTT, 2 mM spermidine, 40 mM Tris (pH 7.9), and 5 mM each NTP, which was incubated at 37 °C for 2.5 h. Then 0.1 U/μL Turbo DNase was added, and the incubation was continued for 1 h. The reaction products were ethanol precipitated, and the RNAs were purified by PAGE and subsequent ethanol precipitation.

The S1-derived RNA pool was used to select aptamiRs that bind pre-miR-155, and the S2-derived pool was used to select aptamiRs that bind either pre-miR-10b or pre-miR-33a. Either a 300- or 500-μL reaction mixture (for S1 or S2, respectively), containing either 1 or 2 nmol RNA (for S1 or S2, respectively), 150 mM NaCl, and 25 mM Tris (pH 7.6), was heated at 70 °C for 1 min and then slowly cooled to 23 °C. An equal volume of a solution containing either 20 or 10 mM MgCl$_2$ (for S1 or S2, respectively), 150 mM NaCl, 25 mM Tris (pH 7.6), and 0.1% TWEEN-20 was added, and the combined mixture was incubated with 1 mg Dynabeads that had been preblocked with tRNA at 23 °C for 1 h. The beads were discarded to remove bead-binding RNAs. Then either 200 pmol L-pre-miR-155 or 100 pmol each of L-pre-miR-10b and L-pre-miR-33a (for S1 or S2, respectively; Figure 1a) were added to the supernatant. The mixture was incubated at 23° for 30 min before adding 2 mg Dynabeads. After shaking at 23 °C for 15 min, the beads were washed four times with a 1-mL solution containing either 10 or 5 mM MgCl$_2$ (for S1 or S2, respectively), 150 mM NaCl, 25 mM Tris (pH 7.6), and 0.1% TWEEN-20. Then the bound RNAs were eluted with two 200-μL volumes of a solution containing 25 mM NaOH and 1 mM EDTA.

The eluted material was neutralized with 1 M Tris (pH 7.6) and ethanol precipitated, and then the RNAs were reverse transcribed in a 100-μL reaction mixture containing 1 μM of either Rev1 or Rev2 (for S1 or S2, respectively), 10 U/μL Superscript II reverse transcriptase, 3 mM MgCl$_2$, 75 mM KCl, 50 mM Tris (pH 8.3), and 0.25 mM each dNTP. After 1 h at 42 °C, the enzyme was inactivated by heating the mixture at 70 °C for 5 min. The cDNAs were amplified by PCR using either Fwd1 and Rev1 (for S1) or Fwd2 and Rev2 (for S2), and the

resulting dsDNAs were used to transcribe RNAs to begin the next round of *in vitro* selection.

The lineage to select D-RNAs that bind either L-pre-miR-10b or L-pre-miR-33a was carried out for 4 rounds with both targets present, and then the population was split and the two pre-miRs were targeted separately in subsequent rounds. The amounts of pool and target RNA, respectively, were decreased progressively: 300 and 50 pmol in round 2, 100 and 50 pmol in rounds 3 and 4, 50 and 25 pmol in round 5, and 30 and 15 pmol in round 6. The L-pre-miR-33a lineage was carried out for a seventh round, using 15 and 10 pmol of pool and target RNA, respectively. The duration of the washing steps was increased over successive rounds, starting with 5 min in the first round and progressing to 2 h by the final round. The lineage to select D-RNAs that bind L-pre-miR-155 was carried out for 6 rounds. The amount of pool RNA was decreased progressively: 500 pmol in round 2, and 300 pmol in rounds 3−6. The duration of the washing steps was increased progressively, as mentioned above.

A branched lineage was initiated starting with material obtained after the first round of selection for binding to L-pre-miR-155, but progressing toward more physiological conditions and selecting for binding to extended-length L-pre-miR-155 (Figure 1a). The procedure was the same as mentioned above, except that the temperature was 37 °C and the concentration of MgCl$_2$ was decreased progressively: 20 mM in rounds 2−4, 5 mM in round 5, and 2 mM in rounds 7−11. The amounts of pool and target RNA, respectively, were decreased progressively: 500 and 200 pmol in round 2, 300 and 100 pmol in round 3, 200 and 100 pmol in round 4, 300 and 100 pmol in round 5, 100 and 50 pmol in rounds 6−8, 300 and 50 pmol in round 9, and 100 and 50 pmol in rounds 10−11. Error-prone PCR[15] was performed after rounds 4 and 7 to introduce additional mutations to the population.

After the final round of each selection, the dsDNAs were cloned into *E. coli* using the TOPO TA Cloning Kit (Life Technologies). The bacteria were grown for 16 h at 37 °C on LB agar plates containing 50 μg/mL carbenicillin. Individual colonies were amplified by PCR and sequenced by Genewiz Inc. (La Jolla, CA) (Figure S1).

Preparation of D-pre-miRs. Full-length D-pre-miRs were prepared by ligation of two synthetic oligonucleotides. For pre-miR-10b these were 5′-UACCCUGUAGAACCGAAUUUGUGUGGUAUCCG-3′ and 5′-pUAUAGUCACAGAUUCGAUUCUAGGGGAAU-3′; for pre-miR-133a these were 5′-GUGCAUUGUAGUUGCAUUG-CAUGUUCUGGUGG-3′ and 5′-pUACCCAUGCAAUGUUUCCA-CAGUGCAUCAC-3′; and for pre-miR-155 these were 5′-UUAA-UGCUAAUCGUGAUAGGGGUUUUGCC-3′ and 5′-pUCCAA-CUGACUCCUACAUAUUAGCAUUAACA-3′. A 500-μL reaction mixture containing 5 nmol each of the two RNAs, 10 mM MgCl$_2$, 1 mM DTT, and 50 mM Tris (pH 7.5) was heated at 70 °C for 1 min and then slowly cooled to 23 °C. Then 400 U/μL T4 RNA ligase was added, and the mixture was incubated at 23 °C for 2 h. The reaction products were ethanol precipitated, and the ligated RNAs were purified by PAGE and subsequent ethanol precipitation.

Electrophoretic Mobility-Shift Assay (EMSA). Dissociation constants of the pre-miR−aptamiR complexes were determined by EMSA, as described previously.[8] 0.1 nM $[5′\text{-}^{32}P]$-labeled D-pre-miR RNA was incubated with various concentrations of L-aptamiR in the presence of either 0.5 or 5 mM MgCl$_2$, 150 mM NaCl, 25 mM Tris (pH 7.6), and 0.1 mg/mL tRNA for 30 min at either 23 or 37 °C. Samples were loaded on a 10% nondenaturing polyacrylamide gel (29:1 acylamide:bis-acrylamide) that had been preheated to the incubation temperature and contained either 0.5 or 5 mM MgCl$_2$, 50 mM NaOAc, and 10 mM Tris (pH 7.6). The current was maintained at <50 mA during the electrophoresis. Bound and unbound D-pre-miR RNAs were quantified using a PharosFX Plus Molecular Imager (BioRad, Hercules, CA). K_d values were determined by fitting the data to the equation: $F_{\text{bound}} = [\text{aptamiR}]/(K_d + [\text{aptamiR}])$.

Structural Probing by Partial Self-Cleavage. A 50-μL reaction mixture was prepared, containing 20 nM $[5′\text{-}^{32}P]$-labeled D-aptamiR or D-pre-miR RNA, either none or 5 μM unlabeled partner RNA, either 1 mM MgCl$_2$ (for aptamiR-155.2) or 5 mM MgCl$_2$ (for aptamiR-10b, -33a, and -155), 150 mM NaCl, and 25 mM Tris (pH 8.0). The

mixture was incubated at either 37 °C for 24 h (for aptamiR-155.2) or 23 °C for 48 h (for aptamiR-10b, aptamiR-33a, and aptamiR-155). The products were analyzed by PAGE and quantitated as described above (Figures S2 and S3).

AptamiR Inhibition of Dicer-Mediated Cleavage. Dicer cleavage was carried out in a 20-μL reaction mixture containing 0.1 nM [5′-^{32}P]-labeled pre-miR, various concentrations of aptamiR, 0.4 pmol human Dicer, either 1 mM $MgCl_2$ (for aptamiR-155.2) or 5 mM $MgCl_2$ (for aptamiR-10b, -33a, and -155), 100 mM NaCl, 25 mM Tris (pH 7.6), 10 mM DTT, 200 μg/mL BSA, and 50 μg/mL tRNA. The reactions were quenched by adding a 5-fold volume of 95% formamide/10 mM EDTA. The products were analyzed by PAGE to determine the fraction cleaved at various times. Values for k_{obs} were determined for each concentration of aptamiR based on a linear fit of the data over the first 15% of the reaction. IC_{50} values were obtained by fitting the k_{obs} values to the equation: $k_{obs} = k_{obs\text{-}min} + \{(k_{obs\text{-}max} - k_{obs\text{-}min})/(1 + {}^{[aptamiR]}/_{IC50})\}$, where $k_{obs\text{-}max}$ is the observed rate in the absence of aptamiR and $k_{obs\text{-}min}$ is the calculated rate at infinite aptamiR concentration.

ASSOCIATED CONTENT

Ⓢ Supporting Information

The Supporting Information is available free of charge on the ACS Publications website at DOI: 10.1021/jacs.5b06696.

> Figures showing sequences of selected clones, structural probing of pre-miRs and aptamiRs, binding interactions between pre-miRs and aptamiRs, aptamiR inhibition of Dicer activity (PDF)

AUTHOR INFORMATION

Corresponding Author

*gjoyce@scripps.edu

Present Address

†Department of Chemistry, Texas A&M University, P.O. Box 30012, College Station, TX 77842-3012.

Notes

The authors declare no competing financial interest.

ACKNOWLEDGMENTS

REFERENCES

(1) (a) Bartel, D. P. *Cell* **2009**, *136*, 215−233. (b) Wilson, R. C.; Doudna, J. A. *Annu. Rev. Biophys.* **2013**, *42*, 217−239.

(2) (a) Iorio, M. V.; Croce, C. M. *Carcinogenesis* **2012**, *33*, 1126−1133. (b) Di Leva, G.; Garofalo, M.; Croce, C. M. *Annu. Rev. Pathol.: Mech. Dis.* **2014**, *9*, 287−314.

(3) Bennett, C. F.; Swayze, E. E. *Annu. Rev. Pharmacol. Toxicol.* **2010**, *50*, 259−293.

(4) Krutzfeldt, J.; Rajewsky, N.; Braich, R.; Rajeev, K. G.; Tuschl, T.; Manoharan, M.; Stoffel, M. *Nature* **2005**, *438*, 685−689.

(5) Obad, S.; dos Santos, C. O.; Petri, A.; Heidenblad, M.; Broom, O.; Ruse, C.; Fu, C.; Lindow, M.; Stenvang, J.; Straarup, E. M.; Hansen, H. F.; Koch, T.; Pappin, D.; Hannon, G. J.; Kauppinen, S. *Nat. Genet.* **2011**, *43*, 371−378.

(6) Fabbri, E.; Manicardi, A.; Tedeschi, T.; Sforza, S.; Bianchi, N.; Brognara, E.; Finotti, A.; Breveglieri, G.; Borgatti, M.; Corradini, R.; Marchelli, R.; Gambari, R. *ChemMedChem* **2011**, *6*, 2192−2202.

(7) (a) van Dongen, S.; Abreu-Goodger, C.; Enright, A. J. *Nat. Methods* **2008**, *5*, 1023−1025. (b) Lindow, M.; Vornlocher, H.-P.; Riley, D.; Kornbrust, D. J.; Burchard, J.; Whiteley, L. O.; Kamens, J.; Thompson, J. D.; Nochur, S.; Younis, H.; Bartz, S.; Parry, J.; Ferrari, N.; Henry, S. P.; Levin, A. A. *Nat. Biotechnol.* **2012**, *30*, 920−923.

(8) Sczepanski, J. T.; Joyce, G. F. *J. Am. Chem. Soc.* **2013**, *135*, 13290−13293.

(9) (a) Ashley, G. W. *J. Am. Chem. Soc.* **1992**, *114*, 9731−9736. (b) Garbesi, A.; Capobinanco, M. L.; Colonna, F. P.; Tondelli, L.; Arcamone, F.; Manzini, G.; Hilbers, C. W.; Aelen, J. M.; Blommers, M. J. *Nucleic Acids Res.* **1993**, *21*, 4159−4165.

(10) (a) Kluiver, J.; Poppema, S.; de Jong, D.; Blokzijl, T.; Harms, G.; Jacobs, S.; Kroesen, B. J.; van den Berg, A. *J. Pathol.* **2005**, *207*, 243−249. (b) Faraoni, I.; Antonetti, F. R.; Cardone, J.; Bonmassar, E. *Biochim. Biophys. Acta, Mol. Basis Dis.* **2009**, *1792*, 497−505. (c) Ma, L.; Teruya-Feldstein, J.; Weinberg, R. A. *Nature* **2007**, *449*, 682−688. (d) Ma, L.; Reinhardt, F.; Pan, E.; Soutschek, J.; Bhat, B.; Marcusson, E. G.; Teruya-Feldstein, J.; Bell, G. W.; Weinberg, R. *Nat. Biotechnol.* **2010**, *28*, 341−347.

(11) (a) Rayner, K. J.; Esau, C. C.; Hussain, F. N.; McDaniel, A. L.; Marshall, S. M.; van Gils, J. M.; Ray, T. D.; Sheedy, F. J.; Goedeke, L.; Liu, X.; Khatsenko, O. G.; Kaimal, V.; Lees, C. J.; Fernandez-Hernando, C.; Fisher, E. A.; Temel, R. E.; Moore, K. J. *Nature* **2011**, *478*, 404−407. (b) Horie, T.; Nishino, T.; Baba, O.; Kuwabara, Y.; Nakao, T.; Nishiga, M.; Usami, S.; Izuhara, M.; Sowa, N.; Yahagi, N.; Shimano, H.; Matsumura, S.; Inoue, K.; Marusawa, H.; Nakamura, T.; Hasegawa, K.; Kume, N.; Yokode, M.; Kita, T.; Kimura, T.; Ono, K. *Nat. Commun.* **2013**, *4*, 2883.

(12) (a) Klussmann, S.; Nolte, A.; Bald, R.; Erdmann, V. A.; Fürste, J. P. *Nat. Biotechnol.* **1996**, *14*, 1112−1115. (b) Nolte, A.; Klussmann, S.; Bald, R.; Erdmann, V. A.; Fürste, J. P. *Nat. Biotechnol.* **1996**, *14*, 1116−1119.

(13) Soukup, G. A.; Breaker, R. R. *RNA* **1999**, *5*, 1308−1325.

(14) (a) Han, J.; Lee, Y.; Yeom, K. H.; Nam, J. W.; Heo, I.; Rhee, J. K.; Sohn, S. Y.; Cho, Y.; Zhang, B. T.; Kim, V. N. *Cell* **2006**, *125*, 887−901. (b) Zhang, X.; Zeng, Y. *Nucleic Acids Res.* **2010**, *38*, 7689−7697. (c) Michlewski, G.; Guil, S.; Semple, C. A.; Caceres, J. F. *Mol. Cell* **2008**, *32*, 383−393. (d) Lünse, C. E.; Michlewski, G.; Hopp, C. S.; Rentmeister, A.; Caceres, J. F.; Famulok, M.; Mayer, G. *Angew. Chem., Int. Ed.* **2010**, *49*, 4674−4677. (e) Roos, M.; Rebhan, M. A.; Lucic, M.; Pavlicek, D.; Pradere, U.; Towbin, H.; Civenni, G.; Catapano, C. V.; Hall, J. *Nucleic Acids Res.* **2015**, *43*, e9.

(15) Cadwell, R. C.; Joyce, G. F. *Genome Res.* **1992**, *2*, 28−33.

(16) (a) Schmidt, F. J.; Cho, B.; Nicholas, H. B. *Ann. N. Y. Acad. Sci.* **1996**, *782*, 526−533. (b) Cho, B.; Taylor, D. C.; Nicholas, H. B., Jr.; Schmidt, F. J. *Bioorg. Med. Chem.* **1997**, *5*, 1107−1113. (c) Ducongé, F.; Toulmé, J.-J. *RNA* **1999**, *5*, 1605−1614.

(17) (a) Schwoebel, F.; van Eijk, L. T.; Zboralski, D.; Sell, S.; Buchner, K.; Maasch, C.; Purschke, W. G.; Humphrey, M.; Zöllner, S.; Eulberg, D.; Morich, F.; Pickkers, P.; Klussmann, S. *Blood* **2013**, *121*, 2311−2315. (b) Hoellenriegel, J.; Zboralski, D.; Maasch, C.; Rosin, N. Y.; Wierda, W. G.; Keating, M. J.; Kruschinski, A.; Burger, J. A. *Blood* **2014**, *123*, 1032−1039.

(18) Pluthero, F. G. *Nucleic Acids Res.* **1993**, *21*, 4850−4851.